A Comparison of Methods for Calculating the Matrix Block Source Term in a Double Porosity Model

Clarisse Alboin, Jérôme Jaffré, Patrick Joly, Jean Roberts, Christophe Serres

INRIA

INSTITUT NATIONAL DE RECHERCHE EN INFORMATIQUE ET EN AUTOMATIQUE

A comparison of methods for calculating the matrix block source term in a double porosity model

Clarisse Alboin — Jérôme Jaffré — Patrick Joly — Jean Roberts — Christophe Serres

N° 4280

Octobre 2001

THÈME 4

ISSN 0249-6399

A comparison of methods for calculating the matrix block source term in a double porosity model

Clarisse Alboin* , Jérôme Jaffré† , Patrick Joly‡ , Jean Roberts§ , Christophe Serres¶

Thème 4 —Simulation et optimisation
de systèmes complexes
Projets Estime et Ondes

Rapport de recherche n° 4280 —Octobre 2001 —23 pages

Abstract: Contaminant transport in a fractured porous medium can be modeled, under appropriate conditions, with a double porosity model. Such a model consists of a parabolic equation with a coupling term describing contaminant exchange between the fractures, which have high permeability, and the matrix block, which has low permeability. A locally conservative method based on mixed finite elements is used to solve the parabolic problem, and the calculation of the coupling term, which involves the solution of diffusion equations in the matrix blocks, is based on an analytic expression. Numerical experiments show that this analytic method for the coupling term compares favorably to several other methods.

Key-words: Porous medium, fractures, double porosity, mixed finite elements

* Thales, Elancourt, France, Clarisse.Alboin@thales.fr
† Inria-Rocquencourt, BP 105, 78153 Le Chesnay Cedex, France, Jerome.Jaffre@inria.fr
‡ Inria-Rocquencourt, BP 105, 78153 Le Chesnay Cedex, France, Patrick.Joly@inria.fr
§ Inria-Rocquencourt, BP 105, 78153 Le Chesnay Cedex, France, Jean.Roberts@inria.fr
¶ IPSN, Fontenay aux Roses, France, Christophe.Serres@ipsn.fr

Unité de recherche INRIA Rocquencourt
Domaine de Voluceau, Rocquencourt, BP 105, 78153 Le Chesnay Cedex (France)
Téléphone : +33 1 39 63 55 11 —Télécopie : +33 1 39 63 53 30

Une comparaison de méthodes calculant le terme source des blocks matriciels dans un modèle double porosité

Résumé : Le transport de contaminants dans un milieu poreux fracturé peut être modélisé, moyennant certaines conditions, par un modèle double porosité. Un tel modèle consiste en une équation parabolique avec un terme de couplage décrivant l'échange de contaminants entre les fractures, qui ont une perméabilité élevée, et les blocs matriciels, dont la perméabilité est au contraire très faible. Une méthode localement conservative basée sur les éléments finis mixtes est utilisée pour résoudre l'équation parabolique, et le calcul du terme de couplage, qui comprend la résolution d'équations de la diffusion dans les blocks matriciels, est basée sur une expression analytique. Des expériences numériques montrent que cette méthode analytique de calcul du terme de couplage se compare favorablement avec plusieurs autres méthodes.

Mots-clés : Milieu poreux, fractures, double porosité, elements finis mixtes

1 Introduction

The transport in a porous medium of a contaminant dissolved in a single phase fluid is governed by the transportation equation

$$\begin{aligned} \omega \frac{\partial c}{\partial t} + \mathrm{div}(-D\nabla c + \mathbf{u}\, c) &= q_c \\ c(\cdot, 0) &= c^0, \end{aligned} \tag{1}$$

where the unknown c is the concentration of the contaminant dissolved in the fluid; the coefficients ω, D and $\mathbf{u}$ are the porosity of the medium, the diffusion and the Darcy velocity of the fluid, respectively; the right hand side q_c is the contaminant source term; and the initial condition c^0 is the concentration of the contaminant at time $t = 0$.

The Darcy velocity $\mathbf{u}$ is given by the flow equation which is Darcy's law relating the fluid pressure with the Darcy velocity $\mathbf{u}$

$$\mathbf{u} = -K\nabla p \tag{2}$$

together with the law of conservation of mass

$$\mathrm{div}\,\mathbf{u} = q. \tag{3}$$

Here, in Darcy's equation, the effects of gravity have been ignored. The coefficient K is the permeability of the rock; more precisely it is the permeability k divided by the viscoscity μ of the fluid which might be dependent on the concentration. However here we neglect this dependence so that K is constant in time. The elliptic conservation law statess that the fluid is supposed to be incompressible.

By a fracture in the porous medium is meant a very thin portion of the domain with very large permeability; very thin in comparison with the size of the domain and very permeable in comparison with the surrounding medium. Here we do not consider specific known fractures that might be included individvually in the model but a network of small interconnected fractures. Also, a certain degree of regularity in the fracture network is assumed. Aside from the fact that we do not have precise information about the form or location of such a network, the difficulty for numerical modeling is a problem of scale. The scale of the fracture width and the scale of the distance between fractures in the network are very small compared to the scale of the domain size. A model that could see this kind of detail would be prohibitively large for performing calculations. However one can not neglect these fractures. There is again a difference in scale in the permeability of the fractures and the permeability of the neighboring domain so that the Darcy velocity is much larger in the fractures and they play a major role in the flow in the medium: if, for example, the source term is located in the network of fractures and vanishes after a certain time, in a first stage, the contaminant, in addition to being convected and diffused in the network of fractures, is dispersed by diffusion into the blocks of porous media, called matrix blocks, which act as reservoirs. Then in a second stage, after the concentration of contaminant in the fractures has diminished, the matrix block acts as a source as the contaminant is rediffused into the fracture system. These exchanges between matrix blocks and fractures are very significant and modify the propagation time of the contaminant [1].

These fractures must be taken into account by some sort of averaging process as in a double porosity model. The double porosity model was first described in articles [2, 3], where the model was a phenomenological model deduced from experimentation. The model was later derived via homogenization [4, 5, 6, 7] and is recalled in Section 2. It consists of a transport equation in the homogeneized domain coupled with a diffusion equation through a source term representing exchange between the homogeneized medium and the matrix blocks. Section 3 presents standard locally conservative numerical methods based on lowest order mixed finite elements.

However local conservation is required only in the homogeneized medium, but is not necessary in the matrix blocks. So the core of this paper is devoted to a semi-analytic calculation of the source term in the matrix blocks in order to decrease computational costs. A similar technique was presented in [8] without the use of an equivalent for small time. Section 4 introduces the analytic expression of the source term describing exchange between the fractures and the matrix blocks. This source term is expressed in terms of a coupling operator which is discretized in time in Section 5. All this is done under the assumption that the permeability is so low that the transport in the matrix block is due only to diffusion. Section 6 contains numerical experiments and some conclusions.

2 The double porosity model

We consider a naturally fractured medium throughout which exists a system of interconnected fracture planes. This medium is idealized as a periodic medium as shown in Figure 1.

Homogenization for this idealized medium is carried out with a parameter ϵ equal to the ratio of the period to the size of the domain. We obtain a medium which has the average properties of the initial medium. The scale of heterogeneities is the microscopic scale and the scale of the homogenized medium is the macroscopic scale. The resulting model is composed of a concentration equation in a homogenized medium to which has been added a source term or a coupling term whose value at point x and time t is obtained by solving a diffusion equation in a matrix block associated with x. The solution acts in turn through a boundary condition as a source for the microscopic model in the matrix block. This model is the double porosity model. Two sets of parameters describe the homogenized medium: macroscopic parameters derived from the microscopic parameters in the fractures and microscopic parameters in the matrix blocks from which the coupling term is determined.

We denote by x the macroscopic variable in the homogenized medium Ω and by y the microscopic variable in a matrix block $\mathcal{Q}_x^m$ associated with the point x (Figure 2). We use the notation $\mathcal{Q}_x$ for the matrix block $\mathcal{Q}_x^m$ together with the surrounding fracture $\mathcal{Q}_x^f$ (Figure 3).

The calculation of the coupling term involves, at each point $x \in \Omega$ and for each time t, the solution of an equation modeling diffusion in a matrix block.

After homogenization, we obtain the following model: for each t and each $x \in \Omega$,

$$\begin{aligned} &\omega \frac{\partial c}{\partial t} + \operatorname{div}(-D\nabla c + \mathbf{u}\, c) = q_c - \frac{1}{|\mathcal{Q}_x|} \int_{\mathcal{Q}_x^m} \frac{\partial c^m}{\partial t}(x, y, t)\, dy \\ &c(\cdot, 0) = c^0 \end{aligned} \tag{4}$$

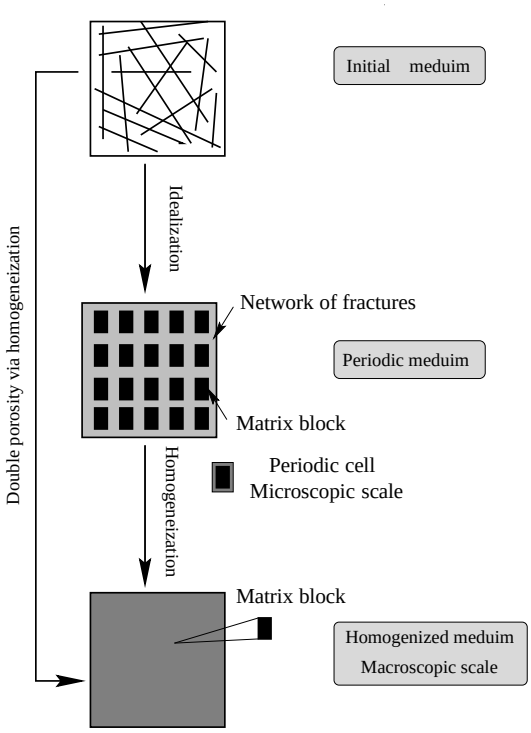

Figure 1: The double porosity model

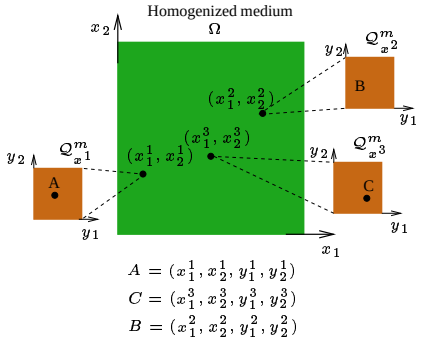

Figure 2: Systems of variables

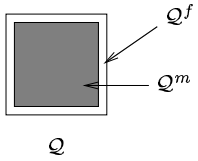

Figure 3: The fracture $\mathcal{Q}^f$ surrounding a matrix bloc $\mathcal{Q}^m$ and $\mathcal{Q} = \mathcal{Q}^m \cup \mathcal{Q}^f$

where the unknown c is the concentration in the homogenized medium. The scalar quantities ω and q_c, respectively the porosity and the given source term in the homogenized medium, are related to the porosity ω^f and the source term q_c^f in the fractures by

$$\omega(x) = \frac{|\mathcal{Q}_x^f|}{|\mathcal{Q}_x|}\omega^f(x) \qquad\qquad q_c(x) = \frac{|\mathcal{Q}_x^f|}{|\mathcal{Q}_x|}q_c^f(x).$$

The vector quantity D in the homogenized medium is related to that in the fractures D^f by

$$D = \frac{1}{|\mathcal{Q}_x|}\int_{|\mathcal{Q}_x^f|}(W(y)+I)dy\ D^f,$$

where $W(y)$ is the n by n matrix $W_{i,j}(y) = \dfrac{\partial w_i}{\partial y_j}$ with w_i the solution to the homogeneous Laplace equation in $\mathcal{Q}_x^f$ with a homogeneous Neuman boundary condition on $\partial\mathcal{Q}_x$ and Neuman boundary condition equal to $-n_j$, minus the j^{th} component of the normal vector on $\partial\mathcal{Q}_x^m$.

The Darcy velocity $\mathbf{u}$ in th e homogenized medium is obtained from

$$\begin{aligned} \mathbf{u} &= -K\nabla p \\ \operatorname{div} \mathbf{u} &= q, \end{aligned} \tag{5}$$

where the permeability K and the source term q in the homogenized medium are given in terms of the corresponding quantities in the fractures, K^f and q^f:

$$K = \frac{1}{|\mathcal{Q}_x|}\int_{|\mathcal{Q}_x^f|}(W(y)+I)dy\ K^f, \qquad q = \frac{|\mathcal{Q}_x^f|}{|\mathcal{Q}_x|}q^f.$$

The term

$$\frac{1}{|\mathcal{Q}_x|}\int_{\mathcal{Q}_x^m}\frac{\partial c^m}{\partial t}(x,y,t)\,dy, \tag{6}$$

is the coupling term which represents the exchange between the fractures and the matrix blocks. The unknown $c^m(x,y,t)$ is the concentration at time t and at point y of the matrix block Q_x associated with x in Ω and is the solution of the contaminant transport equation on the microscopic scale. For $x \in \Omega, c^m(x,\cdot)$ is the solution of a time dependent diffusion equation in $\mathcal{Q}_x^m$:

$$\begin{aligned} &\frac{\partial c^m}{\partial t}(x,y,t) - \alpha(x)\Delta_y c^m(x,y,t) = 0, \quad y \in \mathcal{Q}_x^m, t > 0, \\ &c^m(x,y,0) = 0, \quad y \in \mathcal{Q}_x^m, \\ &c^m(x,y,t) = c(x,t) \quad \text{on } \partial Q_x^m, \end{aligned} \tag{7}$$

where $\alpha(x)$ is the diffusion coefficient in the matrix block Q_x^m. Here the advection term has been neglected as the permeability is assumed to be very low in Q_x^m.

In a numerical model, equation (7) must be solved at each point x of the discretized domain Ω and at each time step which makes calculations with a double porosity model very costly with standard discretization techniques, especially as the low diffusion in the matrix block renders the problem quite stiff. This led us to calculate the coupling term analytically.

3 Numerical Approximation

We have three coupled equations to solve: the flow equation (5) and the transport equation (4) in the homogeneized domain, and the diffusion equation (7) in the matrix blocks. As we have neglected the transport term in the matrix blocks, there is no need to solve for the Darcy velocity there so we do not approximate a flow equation in the matrix blocks.

We discretize the homogeneized domain Ω with a structured mesh of rectangles $C \in \mathcal{T}$ and we denote by $E \in \mathcal{E}$ the edges of the mesh.

Let us consider first, the flow equation (5) in the homogeneized medium Ω which is an elliptic equation. Because of our assumption that the fluid viscocity is not a function of the contaminant concentration, this equation can be solved independently and only has to be solved once. To obtain a precise approximation to the Darcy velocity and to have a locally conservative scheme we use a mixed formulation with the lowest order Raviart-Thomas spaces [9, 10]. The approximate pressure p_h lies in the space M_h of functions constant on each cell $C \in \mathcal{T}$, and the approximate velocity $\mathbf{u}_h$ lies in the space $\mathbf{X}_h$ of vector functions which are bilinear on each cell $C \in \mathcal{T}$ and continuous through the edges $E \in \mathcal{E}$. The degrees of freedom of $\mathbf{u}_h$ are the flow rates through the edges $E \in \mathcal{E}$. Then the approximation equations for equation (5) are

$$\begin{aligned}
&\int_C \mathrm{div}\mathbf{u}_h \, dx = \int_{\partial C} (\mathbf{u}_h \cdot \mathbf{n}_C) dx = 0, \quad C \in \mathcal{T}, \\
&\int_\Omega K^{-1}\mathbf{u}_h \cdot \mathbf{v} \, dx - \int_\Omega p_h \, \mathrm{div}\, \mathbf{v} \, dx + \int_{\partial\Omega} \bar{p} \, \mathbf{v} \cdot \mathbf{n}_\Omega \, ds = 0, \quad \mathbf{v} \in \mathbf{X}_h,
\end{aligned}$$

where $\mathbf{n}_C$ and $\mathbf{n}_\Omega$ are respectively the outward normals to the boundary of C and to that of Ω. Here $\bar{p}$ is a pressure given on the boundary of Ω.

The transport equation (4) in the homogenized medium Ω is a diffusion-advection equation. This is the equation for which local conservation is the most important. We rewrite it as

$$\begin{aligned}
&\omega \frac{\partial c}{\partial t} + \mathrm{div}\,(\mathbf{w} + \mathbf{r}) = \; q_c - \frac{1}{|\mathcal{Q}_x|} \int_{\mathcal{Q}_x^m} \frac{\partial c^m}{\partial t}(x, y, t) \, dy \\
&\mathbf{w}_d = -D\nabla c \\
&\mathbf{w}_a = \mathbf{u}\, c.
\end{aligned} \tag{8}$$

to separate the diffusion contribution from the advection contribution in order to treat these two terms differently. We treat the diffusion term again with a mixed finite element method and the advective term with a first order upstream scheme. Concerning time discretization Δt denotes the time step and we use Euler finite differences, the diffusive term being treated implicitly and the advective term being treated explicitly. On the interval $((n-1)\Delta t, n\Delta t)$ the concentration is approximated by a function $c_h^n \in M_h$ and the vector function $\mathbf{w}_d$ by $\mathbf{w}_{dh}^n \in \mathbf{X}_h$. Then equation (8) is approximated by

$$\int_C \omega \frac{c_h^{n+1} - c_h^n}{\Delta t} \, dx \; + \int_{\partial C} \left(\mathbf{w}_{dh}^{n+1} \, dx \; + (c_h^-)^n \mathbf{u}_h \right) \cdot \mathbf{n}_C \, dx = \int_C \left(q_c - \frac{1}{|\mathcal{Q}_x|} \int_{\mathcal{Q}_x^m} \frac{\partial c^m}{\partial t}(x, y, t) \, dy \right) dx,$$
$$C \in \mathcal{T},$$

$$\int_\Omega D^{-1}\mathbf{w}_{dh} \cdot \mathbf{v}_h \, dx \; - \int_\Omega c_h^{n+1} \, \mathrm{div}\, \mathbf{v}_h \, dx \; + \int_{\partial\Omega} \bar{c}^{n+1} \; \mathbf{v}_h \cdot \mathbf{n}_\Omega \, ds \; = 0, \quad \mathbf{v}_h \in \mathbf{X}_h,$$

where c_h^- denotes the upstream concentration with respect to the velocity $\mathbf{u}_h$ and c_d^{n+1} a given concentration on the boundary of Ω.

Finally the source term (6) must be calculated at each time step and at each point of discretization so we need to solve the matrix block equations (7). In addition to the fact that this equation must be solved $N_t \times M$ times, where N_t is the number of time steps and M the number of discretisation

points, the fact that the coefficient α is in general quite small renders the problem stiff. Standard discretization techniques could be used to approximate the solution of equation (7). However, in order to minimize computational costs, and since local conservation is not necessary for this equation, and since actually only the coupling term (6) is required, we will present an analytical evaluation of it. This is possible since in equation (7) the coefficients as well as the data are constant in space and the geometry of $\mathcal{Q}_x^m$, a rectangle, is simple.

4 Analytic expression of the coupling term

We now give an analytic expression of the coupling term in terms of a convolution kernel written as a series. For simplicity's sake, we have taken $\mathcal{Q}_x^m$ to be a square instead of a general rectangle.

With $\hat{c}^m(x,y,t) = c^m(x,y,t) - c(x,t)$, $\hat{c}^m$ is the solution of

$$\begin{aligned}
&\frac{\partial \hat{c}^m}{\partial t}(x,y,t) - \alpha(x)\Delta_y \hat{c}^m(x,y,t) \;=\; \frac{\partial c}{\partial t}(x,t), \quad y \in \mathcal{Q}_x^m,\ t>0,\\
&\hat{c}^m(x,y,0) \;=\; -c(x,0) \ \text{ in } \mathcal{Q}_x^m\\
&\hat{c}^m(x,y,t) \;=\; 0 \quad \text{ on } \partial\mathcal{Q}_x^m.
\end{aligned}$$

If $\mathcal{Q}_x^m$ is identified with $[-\frac{k}{2},\frac{k}{2}]^2$, the function $\hat{c}^m$ may be expressed in terms of the spectral basis $\{\omega_{p,q} \,:\, p,q \,=\, 1,2,\cdots\}$, where $\omega_{p,q}(y) = \omega_p(y_1)\omega_q(y_2)$ and ω_p is the solution on $[-\frac{h}{2},\frac{h}{2}]$ of

$$-\omega_p'' = \frac{\pi^2 p^2}{k^2}\omega_p, \qquad \omega_p(-\frac{k}{2}) = \omega_p(\frac{k}{2}) = 0,$$

with coefficients $\hat{c}_{p,q}^m$ solutions of the ordinary differential equation

$$\frac{\partial \hat{c}_{p,q}^m}{\partial t}(x,t) + \alpha_{p,q}\hat{c}_{p,q}^m(x,t) = -\frac{\partial c}{\partial t}(x,t)\mu_{p,q},$$

with

$$\alpha_{p,q} = \frac{\alpha\pi^2}{k^2}(p^2+q^2) \qquad \text{and} \qquad \mu_{p,q} = \int_{\mathcal{Q}_x^m} \omega_{p,q}. \tag{9}$$

Thus we have

$$\hat{c}^m(x,y,t) = \sum_{p,q\geq 1} \hat{c}_{p,q}^m(x,t)\omega_{p,q}(y), \tag{10}$$

with

$$\omega_p(y_i) = \begin{cases} \sqrt{\frac{2}{k}}\sin(\frac{p\pi y_i}{k}) & \text{if } p \text{ is even}\\ \sqrt{\frac{2}{k}}\cos(\frac{p\pi y_i}{k}) & \text{if } p \text{ is odd,} \end{cases} \qquad i=1,2,$$

and

$$\hat{c}^m_{p,q}(x,t) = -\mu_{p,q}\left(\int_0^t \frac{\partial c}{\partial t}(x,s)e^{-\alpha_{p,q}(t-s)}ds + c(x,0)e^{-\alpha_{p,q}t}\right).$$

A simple calculation then shows that the coupling term is given by

$$\int_{\mathcal{Q}^m_x} \frac{\partial c^m}{\partial t}(x,y,t)\,dy = \sum_{p,q}\mu^2_{p,q}\alpha_{p,q}\left(\int_0^t \frac{\partial c}{\partial t}(x,s)e^{-\alpha_{p,q}(t-s)}ds + c(x,0)e^{-\alpha_{p,q}t}\right),$$

or, defining the convolution kernel $K_\alpha(t)$,

$$K_\alpha(t) = \sum_{p,q}\mu^2_{p,q}\alpha_{p,q}e^{-\alpha_{p,q}t}, \tag{11}$$

by

$$\int_{\mathcal{Q}^m_x} \frac{\partial c^m}{\partial t}(x,y,t)\,dy = \int_0^t \frac{\partial c}{\partial t}(x,s)K_\alpha(t-s)ds + c(x,0)K_\alpha(t) \tag{12}$$

Even though we have an analytic expression for $S_\alpha(c)$ we do not have a closed form expression. Thus in addition to deciding whether this term should be treated implicitly or explicitly we must approximate the time intergral in the convolution term, approximate the time derivative in this term, and approximate the convolution kernel which is given as an infinite sum. We first investigate some of the properties of the kernel K_α and of the operator S_α.

Lemma 1 *The series, K_α converges on $[0,+\infty)$ and converges uniformly on the subinterval $[\varepsilon,+\infty)$ for each $\varepsilon > 0$. Moreover K_α has the following behavior, for $\alpha \in \mathbb{R}^+$ given,*

$$K_\alpha(t) = 4\sqrt{\frac{|\mathcal{Q}^m|\alpha}{\pi t}} - \frac{16\alpha}{\pi} + O(t). \tag{13}$$

PROOF:
First, calculating that

$$\mu_{p,q} = \begin{cases} \pm\dfrac{8}{pq\pi^2} & \text{if } p \text{ and } q \text{ are odd} \\ 0 & \text{otherwise} \end{cases},$$

we see that $\mu^2_{p,q}\alpha_{p,q} \le \dfrac{128\alpha}{\pi^2}$. Thus

$$K_\alpha(t) \le \frac{128\alpha}{\pi^2}\sum_{p,q\ge 1} e^{-\alpha_{p,q}t} \le \frac{128\alpha}{\pi^2}e^{-2\alpha\pi^2 t},$$

and we see that $K_\alpha(t)$ is a series that converges on $[0,\infty)$ and converges uniformly on $[\varepsilon,\infty)$ for each positive ε.

Then a straightforward calculation shows that

$$K_\alpha(t) = -2\zeta(t)\zeta'(t) \qquad \text{with} \qquad \zeta(t) = \sum_{p\geq 1} \mu_p^2 e^{-\alpha\pi^2 p^2 t}.$$

One can now rewrite $\zeta(t)$ as follows:

$$\zeta(t) \;=\; \int_{-\frac{k}{2}}^{\frac{k}{2}} z(y,t)\, dy,$$

where $z(y,t)$ is the solution of

$$\begin{aligned} &\frac{\partial z}{\partial t} - \alpha \frac{\partial^2 z}{\partial y^2} \;=\; 0, \quad -k/2 \leq y \leq k/2, \\ &z(y,0) \;=\; -1, \qquad -k/2 \leq y \leq k/2, \\ &z(\pm k/2, t) \;=\; 0. \end{aligned}$$

Then $z(y,t)$ can be identified with the restriction to the segment $[-k/2, k/2]$ of the solution $\tilde{z}(y,t)$ of

$$\begin{aligned} &\frac{\partial \tilde{z}}{\partial t} - \alpha \frac{\partial^2 \tilde{z}}{\partial y^2} = 0, \quad y \in \mathbb{R},\ t > 0, \\ &\tilde{z}(y,0) = \sum_{l=-\infty}^{l=\infty} (-1)^{l+1}\, \chi(y - lk), \quad y \in \mathbb{R}. \end{aligned}$$

One may also write $\tilde{z}(y,t)$ as an infinite sum:

$$\tilde{z}(y,t) \;=\; \sum_{l=-\infty}^{l=\infty} (-1)^{l+1} z_l(y,t)$$

with $z_l(y,t)$ the solution of

$$\begin{aligned} &\frac{\partial z_l}{\partial t} - \alpha \frac{\partial^2 z_l}{\partial y^2} = 0, \quad y \in \mathbb{R},\ t > 0, \\ &z_l(y,0) = \chi(y - lk), \quad y \in \mathbb{R}; \end{aligned}$$

that is

$$z_l(y,t) \;=\; \frac{1}{2\sqrt{\pi\alpha t}} \int_{kl-k/2}^{kl+k/2} e^{-\frac{(y-\eta)^2}{4t\alpha}} d\eta.$$

Introducing

$$\zeta_l(t) = \int_{-k/2}^{k/2} z_l(y,t) dy,$$

one has

$$\zeta(t) = \sum_{l=-\infty}^{l=\infty} (-1)^{l+1}\, \zeta_l(t).$$

If $\eta \in [lk - k/2, lk + k/2]$ and $y \in [-k/2, k/2]$, then $k(l-1) \leq \eta - y \leq k(l+1)$, so that

$$|\zeta_l(t)| \leq \frac{k^2}{2\sqrt{\pi\alpha t}}\, e^{-\frac{k^2(l-1)^2}{4t\alpha}}.$$

Thus

$$\begin{aligned}\sum_{l\geq 2} |\zeta_l(t)| &\leq \frac{k^2}{2\sqrt{\pi\alpha t}} \sum_{l\geq 2} e^{-\frac{k^2(l-1)^2}{4t\alpha}} \leq \frac{k^2}{2\sqrt{\pi\alpha t}} \sum_{l\geq 1} e^{-\frac{k^2 l^2}{4t\alpha}} \\ &\leq \frac{k^2}{2\sqrt{\pi\alpha t}}\, e^{-\frac{k^2}{4t\alpha}} \sum_{l\geq 1} e^{-\frac{k^2(l^2-1)}{4t\alpha}}.\end{aligned}$$

Since for $l \geq 1$ we have $l^2 - 1 \geq 2(l-1)$ and we obtain

$$\sum_{l\geq 2} |\zeta_l(t)| \leq \frac{k^2}{2\sqrt{\pi\alpha t}}\, e^{-\frac{k^2}{4t\alpha}} \sum_{l\geq 0} e^{-\frac{2k^2 l}{4t\alpha}} \leq \frac{k^2}{2\sqrt{\pi\alpha t}}\, \frac{e^{-\frac{k^2}{4t\alpha}}}{1 - e^{-\frac{k^2}{2t\alpha}}}.$$

As one clearly has the same upper bound for $\sum_{l\leq -2} |\zeta_l(t)|$ one can conclude that $\sum_{|l|\geq 2} |\zeta_l(t)|$ is $\mathcal{C}^\infty$ on $[0, \infty)$ with all of its derivatives vanishing at 0.

We next consider ζ_1 and ζ_{-1}. The function ζ_1 is given by

$$\zeta_1(t) = \frac{1}{2\sqrt{\pi\alpha t}} \int_{-k/2}^{k/2} \int_{k/2}^{3k/2} e^{-\frac{(y-\eta)^2}{4t\alpha}}\, d\eta\, dy$$

or, denoting by u and v respectively, $\eta - y$ and $\eta + y$,

$$\begin{aligned}\zeta_1(t) &= \frac{1}{4\sqrt{\pi\alpha t}} \left[\int_0^k \int_{k-u}^{k+u} e^{-\frac{u^2}{4t\alpha}}\, dv\, du + \int_k^{2k} \int_{-k+u}^{3k-u} e^{-\frac{u^2}{4t\alpha}}\, dv\, du \right] \\ &= \frac{1}{2\sqrt{\pi\alpha t}} \left[\int_0^k e^{-\frac{u^2}{4t\alpha}} u\, du - \int_k^{2k} e^{-\frac{u^2}{4t\alpha}} (u - 2k)\, du \right].\end{aligned}$$

Now letting $u = \sqrt{t\alpha}\, s$ one obtains

$$\zeta_1(t) = \frac{1}{2\sqrt{\pi\alpha t}} \left[t\alpha \int_0^{\frac{k}{\sqrt{t\alpha}}} e^{-\frac{s^2}{4}} s\, ds - \sqrt{t\alpha} \int_{\frac{k}{\sqrt{t\alpha}}}^{\frac{2k}{\sqrt{t\alpha}}} e^{-\frac{s^2}{4}} (\sqrt{t\alpha} s - 2k)\, ds \right].$$

Thus, as

$$\int_0^{\frac{k}{\sqrt{t\alpha}}} e^{-\frac{s^2}{4}} s\, ds = -2(e^{-\frac{k^2}{4t\alpha}} - 1)$$

and

$$\begin{aligned}\left| \int_{\frac{k}{\sqrt{t\alpha}}}^{\frac{2k}{\sqrt{t\alpha}}} e^{-\frac{s^2}{4}} (\sqrt{t\alpha}s - 2k) ds \right| &\leq e^{-\frac{k^2}{4t\alpha}} \left| \int_{\frac{k}{\sqrt{t\alpha}}}^{\frac{2k}{\sqrt{t\alpha}}} e^{-\frac{s^2}{4}} (\sqrt{t\alpha}s - 2k) ds \right| \\ &\leq e^{-\frac{k^2}{4t\alpha}} \frac{3k^2}{2\sqrt{t\alpha}},\end{aligned}$$

one can conclude that $\zeta_1(t) - \sqrt{\frac{t\alpha}{\pi}}$ is $\mathcal{C}^\infty$ on $[0, \infty)$ with all of its derivatives vanishing at 0. Similarly one may show that $\zeta_{-1}(t) - \sqrt{\frac{t\alpha}{\pi}}$ is $\mathcal{C}^\infty$ on $[0, \infty)$ with all of its derivatives vanishing at 0.

There remains to calculate ζ_0:

$$\zeta_0(t) = \frac{1}{2\sqrt{\pi\alpha t}} \int_{-k/2}^{k/2} \int_{-k/2}^{k/2} e^{-\frac{(y-\eta)^2}{4t\alpha}} d\eta\, dy.$$

With u and v as before one has

$$\begin{aligned}\zeta_0(t) &= \frac{1}{\sqrt{\pi\alpha t}} \left[\int_0^k \int_0^{k-u} e^{-\frac{u^2}{4t\alpha}} dv\, du + \int_k^{2k} \int_{u-k}^{3k-u} e^{-\frac{u^2}{4t\alpha}} dv\, du \right] \\ &= \frac{1}{\sqrt{\pi\alpha t}} \left[\int_0^k k e^{-\frac{u^2}{4t\alpha}} du - \int_0^k e^{-\frac{u^2}{4t\alpha}} u\, du \right].\end{aligned}$$

We note that

$$\int_0^k e^{-\frac{u^2}{4t\alpha}} u\, du = 2\alpha t \left(1 - e^{-\frac{1}{4t\alpha}}\right).$$

As before letting $u = \sqrt{t\alpha}\, s$ one obtains

$$\int_0^k k e^{-\frac{u^2}{4t\alpha}} du = k\sqrt{t\alpha} \left(\int_0^\infty e^{-\frac{s^2}{4}} ds - \int_{\frac{k}{\sqrt{t\alpha}}}^\infty e^{-\frac{s^2}{4}} ds \right).$$

Now, as

$$\int_0^\infty e^{-\frac{s^2}{4}} ds = \sqrt{\pi}$$

and

$$\int_{\frac{k}{\sqrt{t\alpha}}}^{\infty} e^{-\frac{s^2}{4}} ds \geq \int_{\frac{k}{\sqrt{t\alpha}}}^{\frac{2k}{\sqrt{t\alpha}}} \geq e^{-\frac{k^2}{t\alpha}} \frac{k}{\sqrt{t\alpha}},$$

one obtains

$$\int_0^k k e^{-\frac{u^2}{4t\alpha}} du \leq k\sqrt{t\alpha} \left(\sqrt{\pi} - e^{-\frac{k^2}{t\alpha}} \frac{k}{\sqrt{t\alpha}} \right).$$

and $\zeta_0(t) - k + 2\sqrt{\frac{t\alpha}{\pi}}$ is $\mathcal{C}^\infty$ on $[0, \infty)$ vanishing along with all of its derivatives at 0.

Thus one may conclude that $\zeta(t) + k - 4\sqrt{\dfrac{t\alpha}{\pi}}$ is $\mathcal{C}^\infty$ on $[0, \infty)$ vanishing along with all of its derivatives at 0.

The following lemma describes the behaviour of $K_\alpha(t)$ for large t.

Lemma 2 *As t increases away from 0, the kernel K_α decreases rapidly,*

$$K_\alpha(t) \leq C\, e^{\frac{-2\alpha\pi^2 t}{|\Omega^m|}}. \tag{14}$$

This lemma is an immediate consequence of the definition of the kernel (11),(9).

In practice, expression (13) for K_α is very useful for evaluating K_α in a neighborhood of the singularity at 0 since the series in (11) converges very slowly for small t. Estimate (14) indicates that, for large t, calculating only a few terms of this series is sufficient.

As in [11] one can express the coupling term (12) in terms of a coupling operator S_α. For α a function from Ω to $\mathbb{R}^+$, let $\mathcal{S}_\alpha$ be the operator

$$\begin{array}{rccc} \mathcal{S}_\alpha \ : & H^1(0,T;L^2(\Omega)) & \longrightarrow & L^2(0,T;L^2(\Omega)) \\ & c & \longrightarrow & \mathcal{S}_\alpha(c) \end{array} \tag{15}$$

where

$$\mathcal{S}_\alpha(c)(x,t) = \int_0^t \frac{\partial c}{\partial t}(x,s) K_\alpha(t-s) ds + c(x,0) K_\alpha(t).$$

With this notation, problem (4) can be rewritten as follows:

$$\begin{array}{l} \dfrac{\partial c}{\partial t} + \mathrm{div}_x[-D(x)\nabla_x c + u(x)c] + \mathcal{S}_\alpha(c) \ = \ q_c \\ c(x,0) \ = \ c^0(x). \end{array} \tag{16}$$

Remark 1 *As in [12], one can show that the operator $\mathcal{S}_\alpha$ is pseudo-differential in time of order $1/2$, in the sense that, for all $s < \frac{1}{2}$,*

$$\mathcal{S}_\alpha \ : \ H^s(\mathbb{R}^+; L^2(\Omega)) \longrightarrow H^{s-\frac{1}{2}}(\mathbb{R}^+; L^2(\Omega)).$$

Remark 2 *The operator, $\mathcal{S}_\alpha$, is also semi-positive in the sense that for almost every $x \in \Omega$*

$$\int_0^T \mathcal{S}_\alpha(c)(x,s)c(x,s)ds \geq 0. \tag{17}$$

Another usefull property is that

$$\int_0^T \mathcal{S}_\alpha(c)(x,s)\frac{\partial c(x,s)}{\partial s}ds \geq 0. \tag{18}$$

Either of (17) and (18) suffices to show that problem (16) is well posed.

5 Numerical approximation of the coupling operator

5.1 Time discretization

Let $\Delta t = \dfrac{T}{N_t}$, T the final time of the experiment, be the the length of the time step in the homogenized medium. The semi-discretization in time of equation (16) is given by

$$\frac{c^{n+1} - c^n}{\Delta t} + \operatorname{div}(-D\nabla c^{n+1} + \mathbf{u}\, c^n) + (S_\alpha c)^{n+\frac{1}{2}} \ = \ q_c^{n+1}, \tag{19}$$

where the approximation $(S_\alpha c)^{n+\frac{1}{2}}$ of the coupling term, at a point $x \in \Omega$, is given by

$$(S_\alpha c)^{n+\frac{1}{2}}(x) = [\sum_{j=0}^{n} K_{nj}(c^{j+1}(x) - c^j(x)) + \ K_n c^0(x)] \ \frac{1}{|\mathcal{Q}_x|}, \tag{20}$$

and where for all $n,\ n = 0, ..., N_t - 1$,

$$\begin{aligned}
K_{nj} &= \int_{n\Delta t}^{(n+1)\Delta t} \int_{j\Delta t}^{(j+1)\Delta t} \frac{K_\alpha(t-s)}{(\Delta t)^2}\, ds\, dt, \quad \forall k = 0, ..., n-1, \\
K_{nn} &= \int_{n\Delta t}^{(n+1)\Delta t} \int_{n\Delta t}^{t} \frac{K_\alpha(t-s)}{(\Delta t)^2}\, ds\, dt\ , \\
K_n &= \int_{n\Delta t}^{(n+1)\Delta t} \frac{K_\alpha(t)}{\Delta t}\, dt.
\end{aligned}$$

This discretization in time is chosen in order to guarantee the stability of the scheme. In fact, the discretization in time of the coupling term satisfies the stability condition

$$\sum_{n=0}^{N_t-1} (\mathcal{S}_\alpha c)^{n+\frac{1}{2}} \frac{c^{n+1}(x) - c^n(x)}{\Delta t} \Delta t \geq 0. \tag{21}$$

This inequality may be checked by setting

$$c_{\Delta t}(x,t) \;=\; \sum_{l=0}^{N_t} c^l(x)\beta_l(t), \tag{22}$$

where β_l is a hat function; i.e. the piecewise linear function on $[0,T]$ determined by $\beta_l(j\Delta t) = \delta_{j,l},\ j = 0,\ldots,N_t$. and noting that

$$\frac{\partial\, c_{\Delta t}}{\partial t}(x,t) \;=\; \sum_{l=0}^{N_t-1} \frac{c^{l+1}(x) - c^l(x)}{\Delta t} \zeta_{l+1/2}(t), \tag{23}$$

where $\zeta_{l+1/2}(t)$ is the characteristic function

$$\zeta_{l+1/2}(t) \;=\; \begin{cases} 1 & \text{on } [l\,\Delta t, (l+1)\Delta t] \\ 0 & \text{otherwise.} \end{cases}$$

From (18), we have

$$\int_0^T \mathcal{S}_\alpha(c_{\Delta t})(x,t) \frac{\partial c_{\Delta t}(x,t)}{\partial t}\, dt \geq 0.$$

If we substitute for $c_{\Delta t}$ and $\dfrac{\partial c_{\Delta t}}{\partial t}$ their expressions given in (22) and (23), we obtain inequality (21).

5.2 Truncation of the kernel K_α

In practice, the expression for $(S_\alpha c)^{n+\frac{1}{2}}(x)$ given in (20) is still not suitable for calculation: the expression for K_α involves an infinite sum. However, for t very large, K_α is sufficiently small (see (14)) that we can replace K_α by 0. We replace the sum $\displaystyle\sum_{j=0}^{n}$ by $\displaystyle\sum_{j=n-M}^{n}$ in (20):

$$(S_\alpha c)_M^{n+\frac{1}{2}}(x) = \left[\sum_{j=n-M}^{n} K_{nj}(c^{j+1}(x) - c^j(x)) + K_n c^0(x) \right] \frac{1}{|\mathcal{Q}_x|}, \tag{24}$$

and M becomes a parameter of approximation. We also point out that though the expression in (20) for $(S_\alpha c)^{n+\frac{1}{2}}(x)$ seems to require the storage in memory of the concentration at each time step, this is in fact not the case as we have set $K_\alpha = 0$ for t large which implies $K_{nk} = 0$ for k not close to n.

We conjecture that the discretized coupling term expressed with the truncated kernel satisfies as well the stability condition

$$\sum_{n=0}^{N_t-1} (\mathcal{S}_\alpha c)_M^{n+\frac{1}{2}} \frac{c^{n+1}(x) - c^n(x)}{\Delta t} \Delta t \geq 0.$$

6 Numerical experiments

We present two numerical experiments. The first numerical experiment validates the numerical model by comparison with the Grisak laboratory experiment. In the second numerical experiment we compare the analytic method presented above with standard space-time discretization methods for the calculation in the matrix blocks.

6.1 The Grisak experiment

This experiment consists in injecting a chloride tracer into a cylinder of quasi-regular fractured porous rock [13]. The fractures are distributed along two orthogonal directions, one parallel to the axis of revolution of the cylinder. The cylinder is saturated with water and the velocity of the fluid is maintained constant and parallel to the axis of revolution of the cylinder. The tracers are injected into the network of fractures at one end of the cylinder, the relative concentration depending on time is measured at the other end of the cylinder. The microscopic parameters, characterizing the rock and the network of fractures are given in Table 1. The period of simulation is 4 days

Parameters	*Matrix block*	*Fracture network*
Darcy velocity ($cm\,s^{-1}$)	0	$3.4375\,10^{-2}$
Longitudinal dispersion (cm)	-	4
Transversal dispersion (cm)	-	0
Molecular diffusion ($cm^2\,s^{-1}$)	$5\,10^{-7}$	$5\,10^{-7}$
Porosity	0.35	-
Fracture aperture (cm)	-	$8\,10^{-3}$
Space between fractures (cm)	-	4

Table 1: Parameter values for Grisak's experiment

discretized with 4500 time steps. Figure 4 shows the calculated relative concentration at the outflow

end of the cylinder and compares it with an analytical solution given in [13] and with experimental measurements. One can observe that there is good agreement of the three curves, especially that calculated with the double porosity model and that calculated from an analytic expression.

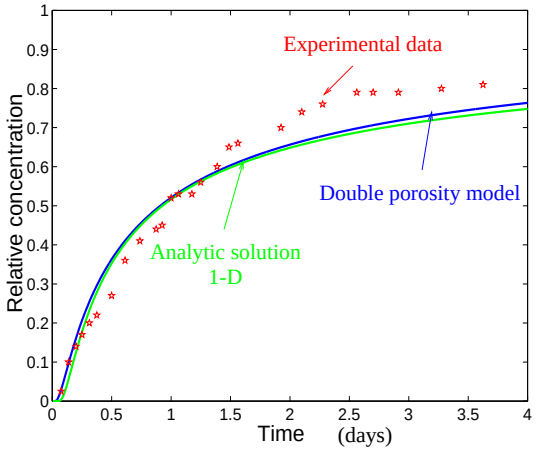

Figure 4: Relative concentrations at the outflow end of the cylinder as functions of time in the Grisak experiment

To illustrate the importance of the coupling term, we simulate the transport of tracers in two cases, when neglecting the coupling term, that is without matrix diffusion, and when taking it into account, that is with matrix diffusion. The results are shown in Figure 5, where the calculated concentrations are shown at a given time, and in Figure 6, where the concentrations at a given point are shown as functions of time. These figures show that for the given data the effect of matrix diffusion is significant. The double porosity model actually smears the contaminant front which would be too sharp if a single porosity model were used.

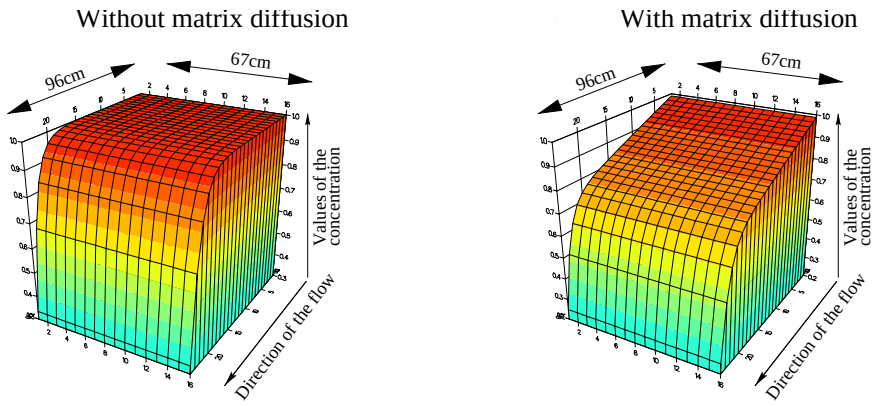

Figure 5: Concentration at 4 days, on a cross-section of the homogenized medium for data given in Table 1

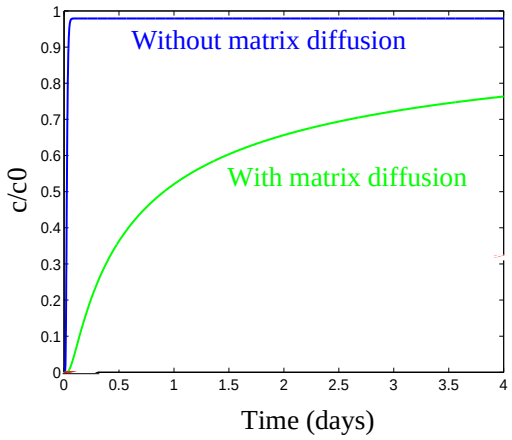

Figure 6: Relative concentration at a point of the homogenized medium for data given in Table 1

6.2 A comparison of different methods for calculating the coupling term

To compare different methods for calculating the coupling term, we consider a simple experiment where a contaminant is transported in a square domain only by diffusion. Initially, we have a positive concentration at the center of the domain. The data for this experiment are given in Table 2. They correspond to a stiff problem, the ratio of the diffusion coefficients in the fracture network to that in the matrix blocks being equal to 100.

Parameters	*Matrix block*	*Fracture network*
Molecular diffusion $(cm^2\ s^{-1})$	10^{-6}	10^{-4}
Porosity	1	1
Fracture aperture (cm)	-	0.1
Space between fractures (cm)	-	10

Table 2: Parameter values for experiments comparing methods of calculating the coupling term

The period of simulation is $4.5\,10^7$ seconds discretized with 900 time steps. We compare the run time and the memory space using four methods to calculate the coupling term: mixed finite elements and cell-centered finite volumes with a uniform grid, a spectral method and the analytic method described above. The first two methods are locally conservative while the two last ones are only globally conservative. However local conservation is important only for the transport equation in the homogeneized medium but not for the calculations in the matrix block which must be only globally conservatives, so the last two methods are also appropriate for the matrix blocks.

One difficulty in this experiment is that in the matrix blocks located where the contaminant front propagates we have to solve a parabolic problem with a large jump between the boundary concentration values and the concentration values inside the matrix block, giving rise to stiff boundary layers (see Figure 7).

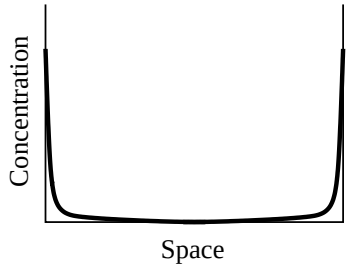

Figure 7: A stiff boundary layer problem arising in some matrix block calculations

For such problems, the mixed finite element method is not appropriate since it does not satisfy the maximum principle and gives oscillations in the neighborhood of the boundary layer, unless a large number of discretization points is put in the boundary layer. With the coarse discretizations that we used it was not possible to get a reasonable answer, and this method was dropped from the comparison.

In Figure 8 we show a comparison between the analytic method, the cell-centered finite volume method with a uniform grid and the spectral method. This comparison shows that the finite volume method is slow to converge which makes it very expensive. On the contrary the spectral method converges quickly since it naturally puts more degrees of freedom close to the boundary. This comparison is somewhat unfair to the finite volume method since one could also use a nonuniform grid with more points close to the boundary. However, even so, as we know, the spectral method would be more acurate, being at its best in a problem like this one – homogeneous, with a simple geometry and constant boundary data.

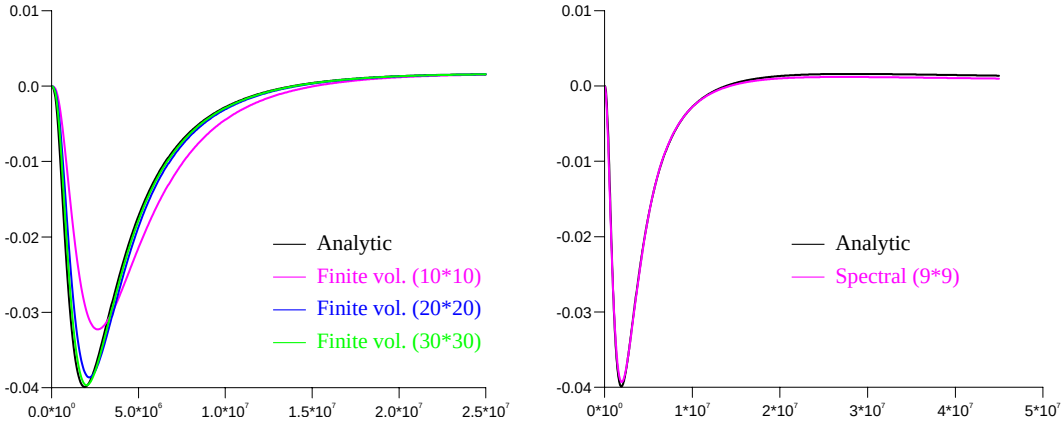

Figure 8: Values of the coupling term as functions of time at some point of the domain Ω for various methods of calculating the coupling term

Table 3 gives a comparison in terms of costs, computing time and memory. The last column gives the relative L^2 error over time of a coupling term calculated in one point by comparison to that calculated analytically, and is a quantitative expression of what is shown if Figure 8. As we can see, the analytical method presented above is much cheaper in terms of computing time. It is somewhat more expensive in terms of memory space since for this stiff problem it is necessary to store the concentration a large number of time steps.

We also looked at a smoother case where the diffusion coefficient in the matrix blocks is now only 10^{-5} (instead of 10^{-6} before) so the the ratio of the diffusion coefficients in the fracture network to that in the matrix blocks is now equal to 10 (instead of 100). The calculation with the analytic method is now cheaper in terms of memory cost than in the stiff case since the number of terms in the sum (24) required to calculate the coupling term is smaller (see Table 4). One should note that in this case a much coarser grid can be used for the finite volume method.

Method	*Run time*	*Memory space*	*Coupling term error*
Finite volumes (10*10)	11'07"	16 Mo	0.28
Finite volumes (20*20)	1h47'	19 Mo	0.1
Finite volumes (30*30)	8h26'	25 Mo	$5\ 10^{-2}$
Spectral method (9*9)	6'31"	16 Mo	$3.46\ 10^{-2}$
Analytical method	2'23"	28 Mo	-

Table 3: Comparison of different methods for calculating the coupling term (stiff case)

Method	*Run time*	*Memory space*	*Coupling term error*
Finite volumes (10*10)	12'49"	16 Mo	$2.8\ 10^{-2}$
Spectral method (9*9)	8'16"	16 Mo	$1.6\ 10^{-2}$
Analytical method	1'04"	19 Mo	-

Table 4: Comparison of different methods for calculating the coupling term (smooth case)

7 Conclusion

In a fractured porous medium with numerous interconnected fractures, the contaminant transfer between matrix blocks and fractures may be very significant. This transfer is taken into account in a double porosity model with a term coupling the homogeneized medium with matrix blocks. We have shown how to calculate this term with an analytical method. Numerical experiments have shown the efficiency of this new numerical procedure compare to standard discretizations which could be used in the matrix blocks .

References

[1] I. Neretnieks. Diffusion in the rock matrix : an important factor in radionuclide retardation. *J. Geophys. Res.*, 85(B8):4379–4397, 1980.

[2] G.I. Barenblatt, I.P. Zheltov, and I.N. Kochina. Basic concepts in the theory of seepage of homogeneous liquids in the fractured rock. *J. Appl. Math. Mech.*, 24:1286–1303, 1960.

[3] J.E. Warren and P.J. Root. The behavior of naturally fractured reservoirs. *Soc. Pet. Eng.*, J. 3:245–255, 1963.

[4] T. Arbogast. Derivation of the double porosity model of single phase flow via homogenization theory. *Siam J. Math. Anal.*, 12(No. 4), July 1990.

[5] J. Douglas and T. Arbogast. Dual porosity models for flow in naturally fractured reservoirs. In J.H Cushman ed., editor, *Dynamics of fluids in hierarchical porous formations*, pages 177–221. Academic press, London, 1990.

[6] U. Hornung and R.E. Showalter. Diffusion models for fractured media. *Journal of Mathematical Analysis and Applications*, 147:69–80, 1990.

[7] A. Bourgeat. Homogenized behavior of diphasic flow in naturally fissured reservoir with uniform fractures. *Comp. Methods in Applied Mechanics and Engeneering*, 47:205–217, 1984.

[8] M. Peszyńska. Finite element approximation of diffusion equations with convolution terms. *Mathematics of Computation*, 65:1019–1037, 1996.

[9] J.E. Roberts and J.-M. Thomas. Mixed and hybrid methods. In P.G. Ciarlet and J.L. Lions, editors, *Handbook of Numerical Analysis Vol.II*, pages 523–639. North Holland, Amsterdam, 1991.

[10] F. Brezzi and M. Fortin. *Mixed and Hybrid Finite Element Methods*. Springer-Verlag, Berlin, 1991.

[11] T. Arbogast. Analysis of the simulation of single phase flow through a naturally fractured reservoir. *SIAM J. Numer. Anal.*, 26:12–29, 1989.

[12] C. Alboin, J. Jaffré, P. Joly, and J.E. Roberts. On a convolution operator arising in a double porosity model. Technical Report 4126, INRIA, BP 105, 78153 Le Chesnay cedex, France, 2001.

[13] G.E. Grisak, J.F. Pickens, and J.A. Cherry. Solute transport through fractured media : 2. column study of fractured till. *Water Resources Research*, 16(4):731–739, 1980.

Unité de recherche INRIA Rocquencourt
Domaine de Voluceau - Rocquencourt - BP 105 - 78153 Le Chesnay Cedex (France)

Unité de recherche INRIA Lorraine : LORIA, Technopôle de Nancy-Brabois - Campus scientifi que
615, rue du Jardin Botanique - BP 101 - 54602 Villers-lès-Nancy Cedex (France)
Unité de recherche INRIA Rennes : IRISA, Campus universitaire de Beaulieu - 35042 Rennes Cedex (France)
Unité de recherche INRIA Rhône-Alpes : 655, avenue de l'Europe - 38330 Montbonnot-St-Martin (France)
Unité de recherche INRIA Sophia Antipolis : 2004, route des Lucioles - BP 93 - 06902 Sophia Antipolis Cedex (France)

Éditeur
INRIA - Domaine de Voluceau - Rocquencourt, BP 105 - 78153 Le Chesnay Cedex (France)
http://www.inria.fr
ISSN 0249-6399